Eur. Phys. J. D **6**, 513–521 (1999)

THE EUROPEAN PHYSICAL JOURNAL D

EDP Sciences

Effects of pump fluctuations on intensity noise of Nd:YVO_4 microchip lasers

A. Bramati[1], J.P. Hermier[1,a], V. Jost[1], E. Giacobino[1], L. Fulbert[2], E. Molva[2], and J.J. Aubert[2]

[1] Laboratoire Kastler Brossel, Université Pierre et Marie Curie, Ecole Normale Supérieure, CNRS, 4, Place Jussieu, 75252, Paris Cedex 05, France
[2] LETI/CEA.G -DOPT, 17, rue des Martyrs, 38054, Grenoble Cedex 9, France

Received: 21 December 1998

Abstract. The principle of pump noise suppression is applied to a Nd:YVO_4 microchip laser, optically pumped by laser diodes. The noise of the microchip laser at low frequency (below the relaxation oscillation frequency) is compared for noisy and amplitude squeezed laser diodes. The minimum intensity noise of the microchip laser is 7 dB above SNL at a frequency of 40 kHz. Very good agreement between experimental results and theoretical predictions of a model based on quantum Langevin equations is found.

PACS. 42.50.Dv Nonclassical field states; squeezed, antibunched, and sub-Poissonian states; operational definitions of the phase of the field; phase measurements – 42.55.Xi Diode-pumped lasers – 42.50.Lc Quantum fluctuations, quantum noise, and quantum jumps

1 Introduction

In recent years, diode-pumped solid-state lasers such as Nd:YAG or Nd:YVO_4 lasers have been overcoming gas lasers for many applications, because of their robustness and reliability [1,2]. However, their noise properties are quite different from those of the gas lasers [3–5]. Their intensity noise is somewhat similar to the one of the semiconductor lasers. Like the semiconductor lasers, they exhibit a large noise peak at high frequency due to the so-called relaxation oscillation. The noise peak is in the gigahertz range for the semiconductor lasers whereas it is in the kilohertz-to-megahertz range for the solid-state lasers, depending on the parameters of the laser cavity. Well above the relaxation oscillation frequency, the intensity noise goes to the standard quantum limit, since it is mainly due to the vacuum fluctuations outside the laser cavity that are reflected off the coupling mirror. For frequencies well below the relaxation oscillation frequency, the intensity noise of the laser is related to the noise of the pump laser [6,7].

For semiconductor lasers, it was demonstrated that intensity squeezed light can be generated when high impedance pump noise suppression is used together with appropriate line narrowing techniques [8–10]. The case of solid-state lasers differs from that of the semiconductor lasers by the pump mechanism, which is optical pumping for solid-state lasers as opposed to electrical pumping for semiconductor lasers. In the present work, our aim is to precisely study the effect of the reduction of the optical pump noise on the intensity noise of solid-state laser and to investigate the possibility to achieve sub-shot noise operation under pump noise suppression. We present an experimental investigation of the intensity noise properties of a Nd:YVO_4 microchip laser pumped by laser diodes having various noise characteristics. More specifically we have compared the effect of pumping with laser diodes exhibiting excess intensity noise, standard intensity quantum noise and sub-shot intensity noise. The sub-shot noise operation of the pump laser is achieved with two different configurations: grating extended cavity and injection locking, respectively. Accurate comparison between theoretical predictions of a full quantum model based on quantum Langevin approach is presented. Our model is based on a microscopic theory of the laser and does not assume any approximation on the evolution time scales of the various quantities involved in the problem. We show that low-frequency noise decreases with pump noise, but we observe a discrepancy at low frequency that cannot be interpreted as due to excess pump noise (contrary to the case of [11]). Agreement between theory and experiment is retrieved when the amplitude of the relaxation oscillation is decreased.

2 Theoretical model

For a theoretical description of the solid-state laser noise properties we have used a full quantum model based on the Langevin equations approach [12]. The model deals with a system of homogeneously broadened two-level atoms with

[a] e-mail: `hermier@spectro.jussieu.fr`

transition frequency ω_{ab}, assuming that the lower level is not the ground state. The atoms fill a resonant cavity of length L and volume V with intensity transmission coefficient of the coupling mirrors T. The atoms interact with the radiation field of a single excited mode of the cavity, which is considered as a plane wave with frequency ω_c. The model is well adapted to describe the behavior of Nd:YVO_4 laser. The laser dynamics is described by the following stochastic c-number Langevin equations:

$$\dot{\mathcal{A}}(t) = -\kappa/2\ \mathcal{A}(t) + g\mathcal{M}(t) + \mathcal{F}_\gamma(t)\,, \tag{1}$$

$$\dot{\mathcal{M}}(t) = -\gamma_{ab}\mathcal{M}(t) + g\left[\mathcal{N}_a(t) - \mathcal{N}_b(t)\right]\mathcal{A}(t) + \mathcal{F}_\mathcal{M}(t), \tag{2}$$

$$\dot{\mathcal{N}}_a(t) = R - (\gamma_a + \gamma'_a)\,\mathcal{N}_a(t) - g\left[\mathcal{A}^*(t)\mathcal{M}(t) + \mathcal{M}^*(t)\mathcal{A}(t)\right] + \mathcal{F}_a(t)\,, \tag{3}$$

$$\dot{\mathcal{N}}_b(t) = -\gamma_b\mathcal{N}_b(t) + \gamma'_a\mathcal{N}_a(t) + g\left[\mathcal{A}^*(t)\mathcal{M}(t) + \mathcal{M}^*(t)\mathcal{A}(t)\right] + \mathcal{F}_b(t)\,. \tag{4}$$

The stochastic c-number variable $\mathcal{A}(t)$ represents the electromagnetic field. $\mathcal{N}_a$ and $\mathcal{N}_b$ represent the macroscopic atomic population of the upper and lower level, respectively. $\mathcal{M}(t)$ represents the macroscopic atomic polarisation. κ is the total cavity damping constant. In the original model, the cavity damping constant was assumed to be equal to the output coupling rate $\kappa_{\rm out}$. Here we have included internal optical losses represented by the rate $\kappa_{\rm losses}$. Subsequently, we have $\kappa = \kappa_{\rm out} + \kappa_{\rm losses}$. γ_a and γ_b are the decay rates of the populations of the upper and lower levels to the other atomic levels; γ'_a is the spontaneous decay rate between the lasing levels and γ_{ab} is the decay rate of the atomic polarisation. R is the mean pumping rate. The coupling constant g is given by

$$g = \sqrt{\frac{1}{2\varepsilon_0\omega_c V}}\,\omega_{ab}\mu\,, \tag{5}$$

where μ is the magnitude of the atomic dipole moment. The functions $\mathcal{F}_k(t)$ with $k = \gamma, \mathcal{M}, a, b$ are the stochastic c-number Langevin forces with the properties:

$$\langle \mathcal{F}_k(t)\rangle = 0\,, \tag{6}$$

$$\langle \mathcal{F}_k(t)\mathcal{F}_l(t')\rangle = 2\mathcal{D}_{kl}\delta(t-t')\,, \tag{7}$$

where $\mathcal{D}_{kl}$ represents the diffusion coefficient for the c-number Langevin force. The nonvanishing diffusion coefficients are given in appendix.

Solving the c-number Langevin equations allows us to calculate the steady-state solutions for the field and atomic variables and to derive the spectra of the fluctuations of the field quadrature components. The steady-state solutions for laser operation above threshold are obtained by dropping the noise terms in equations (1–4) and setting the time derivatives equal to zero. For the mean intensity of the laser field inside the cavity $I_0 = \mathcal{A}_0^2$, we obtain

$$I_0 = I_{\rm s}\left(R/R_{\rm th} - 1\right)\,, \tag{8}$$

where the saturation intensity $I_{\rm s}$ is given by

$$I_{\rm s} = \frac{\gamma_{ab}\gamma_b}{2g^2}\frac{\gamma_a + \gamma'_a}{\gamma_a + \gamma_b}\,, \tag{9}$$

$R_{\rm th}$ is the threshold pumping rate

$$R_{\rm th} = \frac{\kappa\gamma_{ab}\gamma_b}{2g^2}\frac{\gamma_a + \gamma'_a}{\gamma_b - \gamma'_a}\,. \tag{10}$$

The steady-state populations of the upper and lower levels are given by

$$\mathcal{N}_{a0} = \frac{R - \kappa I_0}{\gamma_a + \gamma'_a}\,, \tag{11}$$

$$\mathcal{N}_{b0} = \frac{\gamma'_a R - \kappa\gamma_a I_0}{\gamma_b\left(\gamma_a + \gamma'_a\right)}\,. \tag{12}$$

The steady-state value of the atomic polarisation can be expressed in terms of the mean value of the field

$$\mathcal{M}_0 = \frac{\kappa}{2g}\mathcal{A}_0\,. \tag{13}$$

The evolution of the quantum fluctuations is obtained by linearizing equations (1–4) around the steady-state solution. A Fourier transform of the equations for fluctuations converts the differential equations into algebraic ones. The solutions of the linear system allow to analytically calculate the intensity noise spectrum at the output of the laser as a function of the relaxation constants of the upper and lower levels of the laser transition and of the pump noise.

In the original formulation of [12] the pump noise is described by the parameter p ranging from 0 to 1 ($p = 0$ for Poissonian pump; $p = 1$ for regular pump). In order to reproduce the experimental conditions more precisely, we generalize the model by introducing the spectral density of the pump noise $s(\widetilde{\Omega})$ normalised to the shot noise.

According to [12] and setting $p(\widetilde{\Omega}) = 1 - s(\widetilde{\Omega})$, the normalised intensity noise spectrum at the laser output is given by

$$V_{\rm out}(\widetilde{\Omega}) = 1 + \eta(V_A(\widetilde{\Omega}) - 1)\,, \tag{14}$$

$$\begin{aligned} V_A(\widetilde{\Omega}) = 1 &+ \frac{2bc(a+a')}{b-a'}\frac{1}{D(\widetilde{\Omega})}\left(\left(b^2+\widetilde{\Omega}^2\right)\right. \\ &\times\left[(a+a')^2+\widetilde{\Omega}^2\right]\left[r + n\left(\frac{c}{a+a'} - 1\right)\right] \\ &+2w^2\left\{\left[(b-a')^2+\widetilde{\Omega}^2\right]\left[n+\left(s(\widetilde{\Omega})-1\right)r/2\right]\right. \\ &-\left[(b-a')(a+a')+\widetilde{\Omega}^2\right]\left(r - \frac{a+2a'}{a+a'}n\right) \\ &\left.\left.+\left[(a+a')^2+\widetilde{\Omega}^2\right]\left(\frac{a'}{a+a'} - \frac{b}{c}\frac{b-a'}{a+a'}\right)\right\}\right), \end{aligned} \tag{15}$$

where $\eta = \kappa_{\rm out}/\kappa$ represents the correction for internal optical losses. The dimensionless parameters a, b, c and the dimensionless noise frequency $\widetilde{\Omega}$ are defined as follows:

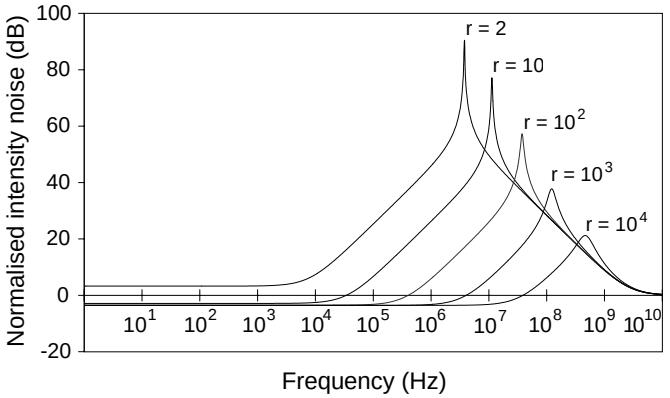

Fig. 1. Calculated normalised intensity noise spectra of the Nd:YVO_4 microchip laser pumped with a noiseless pump ($s(\widetilde{\Omega}) = 0$) with the parameters given in the text for $r = 2$, 10, 100, 1000, 10000.

$a \equiv \gamma_a/\kappa$ (respectively, $b \equiv \gamma_b/\kappa$) is the normalised decay rate of the upper level (respectively, lower level);

$a' \equiv \gamma'_a/\kappa$ is the normalised spontaneous decay rate between the lasing levels;

$c \equiv \gamma_{ab}/\kappa$ is the normalised decay rate of the polarisation;

$\widetilde{\Omega} \equiv \Omega/\kappa$.

Also the following shorthands have been introduced:

$$D(\widetilde{\Omega}) = \left| -i\widetilde{\Omega}\left(\frac{1}{2} + c - i\widetilde{\Omega}\right)\left(b - i\widetilde{\Omega}\right)\left(a + a' - i\widetilde{\Omega}\right) + 2w^2\left(a + b - i2\widetilde{\Omega}\right)\left(1 - i\widetilde{\Omega}\right)\right|^2, \quad (16)$$

$$n = \frac{ra + b + a'(r-1)}{a+b}, \quad (17)$$

$$w^2 = \frac{(a+a')\,bc}{2(a+b)}(r-1)\,. \quad (18)$$

The normalised pump parameter r is defined as the ratio between the pump power p_{pump} and the threshold pump power p_{th}: $r = p_{\mathrm{pump}}/p_{\mathrm{th}}$.

Equation (14) is quite general and does not rely on any adiabatic elimination of variables. It may be used to deal with all types of lasers. In order to gain some physical insight from this formula, we can, however, make some approximations which lead to a simplified expression. The laser under study is a Nd:YVO_4 laser, belonging to a third-class lasers [13], characterized by a decay rate of the atomic polarisation much faster than the other relaxation rates. With respect to the dimensionless variables previously introduced, this condition is written $c \gg 1 \gg a, b, a'$. Applying this approximation to equation (14) is equivalent to perform the adiabatic elimination of the atomic polarization. Moreover, the noise spectrum of these lasers is dominated by the relaxation oscillation (Fig. 1): for low frequencies the noise increases from its minimum value corresponding to zero frequency; for high frequencies, the intensity noise spectrum decreases toward the quantum standard limit.

The minimum intensity noise for the third-class lasers is hence obtained from equation (14) setting $\widetilde{\Omega} = 0$ and $c \to \infty$. For the specific case of the Nd:YVO_4 laser, the condition $b \gg a, a'$ is also verified. This leads to the very simple following formula:

$$V_m(0) \cong 1 - \eta + \eta\left[s + \frac{s+1}{r-1} + \frac{2}{(r-1)^2}\right]. \quad (19)$$

From equation (19) we derive the condition for observing intensity noise below the shot noise level in the laser output:

$$r > \frac{3-s}{1-s} \equiv r_{\mathrm{th}}\,. \quad (20)$$

Equation (20) implies that intensity squeezing can only be observed with a squeezed pump ($s < 1$) and that the laser must operate very far above threshold.

To get the detailed noise properties of the Nd:YVO_4 laser at all frequencies, we use equations (14) and (15). Figure 1 shows the normalised theoretical noise spectra for different values of the normalized pump parameter r, and for a perfectly noiseless pump. The other parameters correspond to the values of our microchip laser and are given in the experimental results section. As can be seen in Figure 1, suppression of the pump noise allows to generate squeezed states.

According to equation (19), the amount of squeezing increases with the pump rate r and it is limited by the quantum efficiency of the laser. The frequency range suitable to observe squeezed light is limited to a low-frequency region well below the relaxation oscillation peak, and it also increases with the pump parameter r, because the relaxation oscillation frequency ($\widetilde{\Omega}_{\mathrm{RO}}$) shifts to higher frequencies, according to the equation:

$$\widetilde{\Omega}_{\mathrm{RO}} \cong \sqrt{(a+a')(r-1)}. \quad (21)$$

The theoretical analysis indicates very clearly the features that the laser has to present in order to generate intensity squeezed light via pump noise suppression. First of all, the laser has to display a very low threshold to achieve far above threshold operation. The laser should also have a high quantum efficiency. Quantum efficiency of the laser may be limited by internal optical losses η and the conversion ratio η_{p} of the photons of the pump beam into lasing photons. These two mechanisms, however, have different effects on the noise properties of the laser. The first one reduces the maximum achievable squeezing, but it does not change the value of r_{th} given by equation (20). In contrast, the second one influences directly the noise of the pump beam (which approaches the shot noise level: $s \to 1$ in equation (20)), increasing the value of r_{th} necessary to generate squeezed light ($r_{\mathrm{th}} \to \infty$ for $\eta_{\mathrm{p}} \to 0$).

Finally, to avoid the competition between oscillating modes, the laser should have single-mode operation. The requirements concerning low threshold and high quantum efficiency imply the use of a laser material with high stimulated emission gain and high pump absorption; the

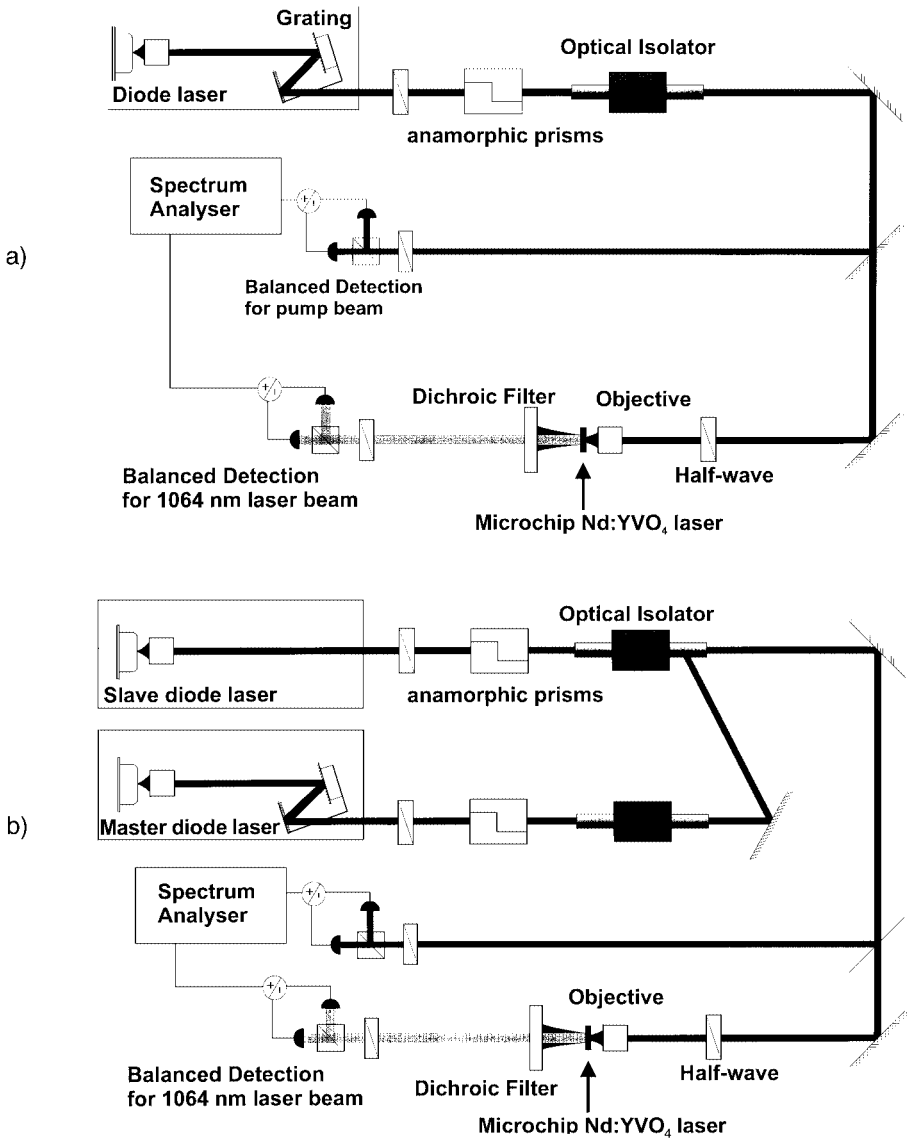

Fig. 2. a) Experimental set-up for noise measurements in a Nd:YVO_4 microchip laser pumped by a grating extended cavity laser diode. b) Experimental set-up for noise measurements in a Nd:YVO_4 microchip laser pumped by an injection locked laser diode.

single-mode operation can be achieved by a laser with a short Fabry-Perot cavity, and a narrow gain curve. The Nd:YVO_4 microchip laser used in our experiment is a good candidate: the high absorption coefficient of 70 cm^{-1} at 808 nm (2% Nd doping) ensures the low threshold (4.2 mW) and good quantum efficiency ($\sim$ 40%); the cavity length of 300 μm together with a narrow gain bandwidth (0.95 nm [14]) ensure the single-frequency oscillation.

3 Experimental set-up

The experimental set-up for noise measurements in Nd:YVO_4 microchip laser is shown in Figures 2a and 2b. The amplitude squeezed laser diode used for optical pumping of solid-state laser is an index guided quantum well GaAlAs laser diode (SDL 5422H1) operating at 810 nm. Noise reduction in the pump beam is achieved by driving the laser diode with a high-impedance constant current source and suppressing the side modes using two different configurations as described in [15], namely feedback from an external grating in an extended cavity laser (Fig. 2a) and injection locking with a master laser (Fig. 2b).

In the external grating configuration a reflection holographic grating is set at a distance of 10 cm from the laser, in Littrow configuration. By tilting the grating, the laser wavelength can be tuned to match the maximum of the Nd:YVO_4 line absorption at 808.5 nm.

In the injection locking set-up, the laser is injected by a master laser which is a grating extended cavity semiconductor laser. The injection locking set-up, with an extended cavity master laser is a device completely tunable over several nanometers, and allows us to match the

frequency of the pump beam with the maximum of the absorption curve of the Nd:YVO_4. In both configurations, astigmatism in the beam is corrected by means of anamorphic prisms. Two optical isolators (for a total isolation of 70 dB) are employed to prevent back reflection into the pump laser. The optical power available for pumping process is 70 mW for the injection locking set-up and 45 mW (due to the losses of the grating) in the grating extended cavity configuration. The intensity noise of the pump laser diode is measured by a standard balanced detection (two high-efficiency EG&G FND100 PIN photodiodes), which allows to measure, under the same conditions, the shot noise and the intensity noise of the laser beam. We performed several tests in order to check the reliability of the shot noise measured in this way, as described in [15]. The common mode rejection of the balanced detection is better than 30 dB in the range of 0–30 MHz; electronic and dark noise are typically more than 10 dB below the shot noise level. The pump beam is sent to the microchip laser by mean of two mirrors and focused into the laser with a $f = 8$ mm objective. The polarisation of the pump beam is fixed by a half-wave plate in order to achieve maximum absorption in the Nd:YVO_4 crystal. The microchip laser is mounted on a xyz-translation stage which allows an optimum alignment.

The Nd:YVO_4 microchip laser is 300 μm long, with a plane-plane monolithic cavity (the stability is ensured by thermal lens effects) in which the mirrors were deposited directly onto the crystal. The output mirror and back reflector have reflectivities of 97% and 99.5%, respectively, at 1.064 μm. The mirrors do not have special coatings for wavelength of pump radiation at 810 nm. Accurate measurements show a reflectivity of 24% and a transmissivity of 7% for pump radiation.

For the intensity noise measurements on the beam emitted by the microchip we used a two-fold experimental set-up. For measurements in low-frequency region (0–300 kHz) we use a balanced detection designed for 1.064 μm. The 1.064 μm light is detected by two high quantum efficiency (90%) InGaAs photodiodes. The electronic devices that complete the balanced detection are analogous to those previously described in [15]. The common mode rejection is better than 30 dB. For measurements at higher frequencies (up to 30 MHz), balanced detection is no longer reliable due to the very high excess noise of the relaxation peak (more than 80 dB) which exceeds the common mode rejection ratio. Therefore in this range of frequencies we performed the noise measurements with one photodiode, and we chose to calibrate the shot noise level with an independent source. For the calibration we use the noise obtained by direct detection on one photodiode of attenuated radiation emitted by a shot noise limited laser diode. It is worth saying that no correction has to be calculated, due to the difference in the wavelength of the two beams. In fact we detect the noise of the photocurrent which is independent of the wavelength. We check carefully linear dependance of the calibrated shot noise signal with the optical power incident on the photodiode. The shot noise obtained in this way was in agreement within 0.1 dB with the noise obtained by a thermal light generating the same DC current on the photodiode.

4 Experimental results

In this section we present the experimental results obtained with the microchip Nd:YVO_4 laser previously described. The pump power at threshold is 4.2 mW, the maximum single TEM_{00} mode power output is 10 mW obtained by pumping with an injection locked laser diode (pump power about 70 mW); in this conditions the normalised pump parameter assumes the value $r \cong 9.5$. If the pump laser is an extended cavity laser the maximum value achievable for r is about 6. In order to make a comparison between the experimental noise spectra and the theoretical predictions, the values of the parameters of the model are set as follows: the decay rate of the upper level γ_a and the spontaneous decay rate between the lasing levels γ'_a for a Nd:YVO_4 crystal doped at 2% are taken from [16, 17]; we set $\gamma_a = 3.3 \times 10^4$ s^{-1} and $\gamma'_a = 3.3 \times 10^3$ s^{-1}. The values of γ_b, decay rate of the lower level, found in the literature [18,16] for Nd:YVO_4 crystal are affected by a huge uncertainty (more than two orders of magnitude); within this range, we choose a value of $\gamma_b = 3 \times 10^9$ s^{-1} that ensures an optimal fit of the experimental curve. The decay rate of the polarisation γ_{ab} is set equal to 7×10^{11} s^{-1} according to [16,17]. The experimental determination of the optical pump power threshold and the measurement of the optical pump power allow us to easily calculate the normalised pump parameter r. The total cavity damping constant κ can be determined by the dependence of the relaxation oscillation frequency on the pump parameter r, according to the equation

$$\Omega_{\mathrm{RO}} = \sqrt{k\,(\gamma_a + \gamma'_a)\,(r-1)}\,, \tag{22}$$

we find $\kappa = 1.56 \times 10^{10}$ s^{-1}. The output coupling κ_{out}, calculated from the reflectivities of the cavity mirrors, is found to be 8.36×10^9 s^{-1}.

We first consider the intensity noise characteristics of the two different pump laser diodes, the grating extended cavity laser diode and the injection locked laser diode. As described in [15] the feedback from grating and injection locking are useful techniques to generate amplitude squeezed light from laser diodes. Figures 3a and 3b show the normalized intensity noise spectra of the grating extended cavity laser diode for low-frequency region (0–300 kHz) and for higher frequencies (0–30 MHz), respectively. After correction for detection efficiency the amount of amplitude squeezing at the laser output is 0.7 dB, flat over the whole frequency range between 1 to 30 MHz. For frequencies lower than 300 kHz the pump laser diode exhibits a slight excess noise (< 3 dB). For frequencies below 50 kHz technical $1/f$ noise increases the excess noise up to 10 dB. Amplitude squeezing of 1.1 dB at the laser output in the range 0–30 MHz is achieved for the injection locked laser; this represents a slight improvement with respect

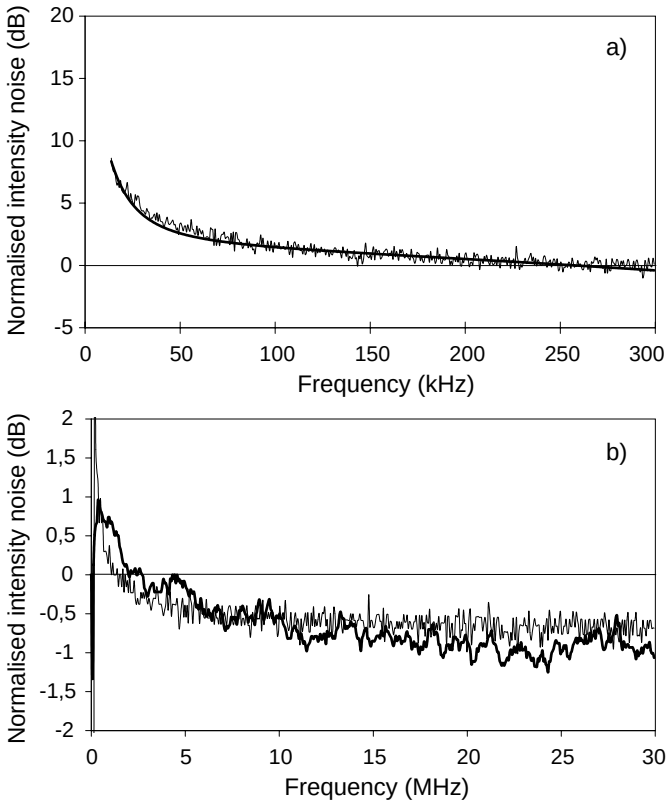

Fig. 3. a) Normalised intensity noise spectrum at the laser output (after correction for detection efficiency) for the grating extended cavity laser diode in the low-frequency region (0–300 kHz). The fit (thick line) is obtained with an empirical expression which is then used to compute the noise shown in Figure 4b. b) Normalised intensity noise spectrum at the laser output (after correction for detection efficiency) for the grating extended cavity laser diode and for the injection locked laser diode (thick line) in the high-frequency region (0–30 MHz).

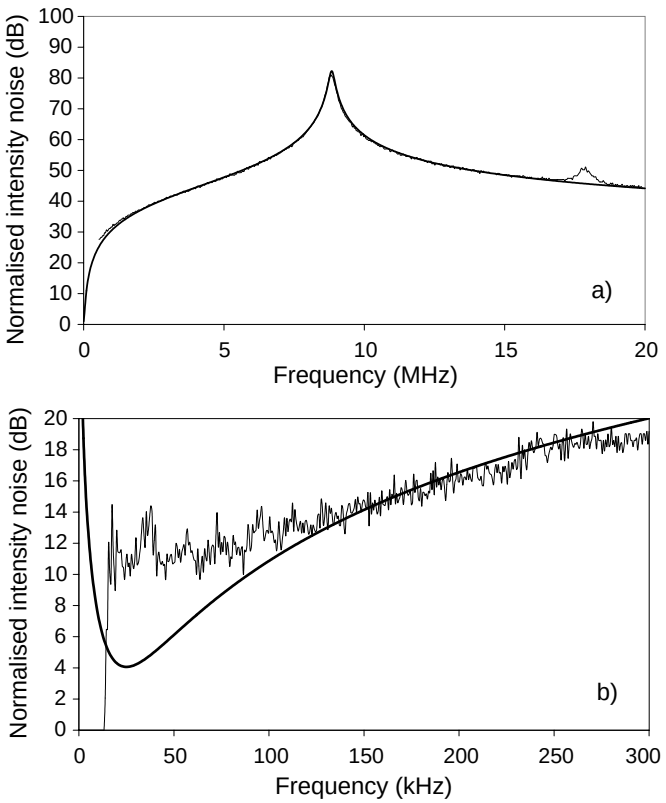

Fig. 4. a) Normalised experimental and theoretical (thick line) intensity noise spectra of the Nd:YVO_4 microchip laser pumped by a grating extended cavity laser diode in the 0–20 MHz frequency range. The corresponding pump noise is shown in Figure 3b. b) Normalised experimental and theoretical (thick line) intensity noise spectra of the Nd:YVO_4 microchip laser pumped by a grating extended cavity laser diode in the 0–300 kHz frequency range. The corresponding pump noise is shown in Figure 3a.

to grating extended cavity laser. The intensity noise spectrum for the low-frequencies region exhibits a behavior similar to that of the grating extended cavity laser.

We will now consider the noise properties of the Nd:YVO_4 microchip laser. All the noise spectra presented in the following are corrected by taking into account the detection efficiency, therefore they display the noise at the output of the laser. Figure 4 shows the normalized intensity noise spectrum of the Nd:YVO_4 microchip laser pumped with the extended cavity laser, with pump noise corresponding to Figure 3. For this measurement the power was about 6 mW and $r = 6$. The theoretical curve (thick line) is obtained from equation (14) with the parameters given in the text; $s(\widetilde{\Omega})$ is given by an empirical expression fitting the measured pump noise (thick line in Fig. 3) and it is corrected for losses experienced by the pump beam (about 40%). The theoretical curve is in good agreement with the experimental one for a very large range of frequencies, particularly around the relaxation oscillation peak, well reproduced by theory (Fig. 4a). However, a significant discrepancy is evident at very low frequencies (below 100 kHz) (Fig. 4b). A minimum noise of 11 dB above shot noise level (SNL) is achieved at frequencies of 30 kHz, whereas the model predicts 5 dB above SNL. In a recent experiment [11] performed on Nd:YVO_4 microchip laser pumped by an amplitude squeezed injection locked laser diode, an analogous discrepancy between theoretical predictions and experimental results is observed in low-frequency range. The authors assumed that the low-frequency extra noise could originate from the spectral distribution of the intensity squeezed light of the injection locked pump laser diode that they use in the experimental set-up. In fact, in the case of the injection locked laser, the main mode can exhibit excess noise even if the total intensity noise is squeezed [19]. This excess noise typically ranges from 1 to 10 dB, depending on the optimisation of the injection parameters such as alignment, injected power, master frequency. As the microchip laser, due to its absorption linewidth of 1 nm, is pumped only by the main mode and few longitudinal side modes, it could experience excess pump noise.

However, this explanation does not hold in our case. We have checked that in the grating extended cavity configuration, as explained in [19], no difference is observed

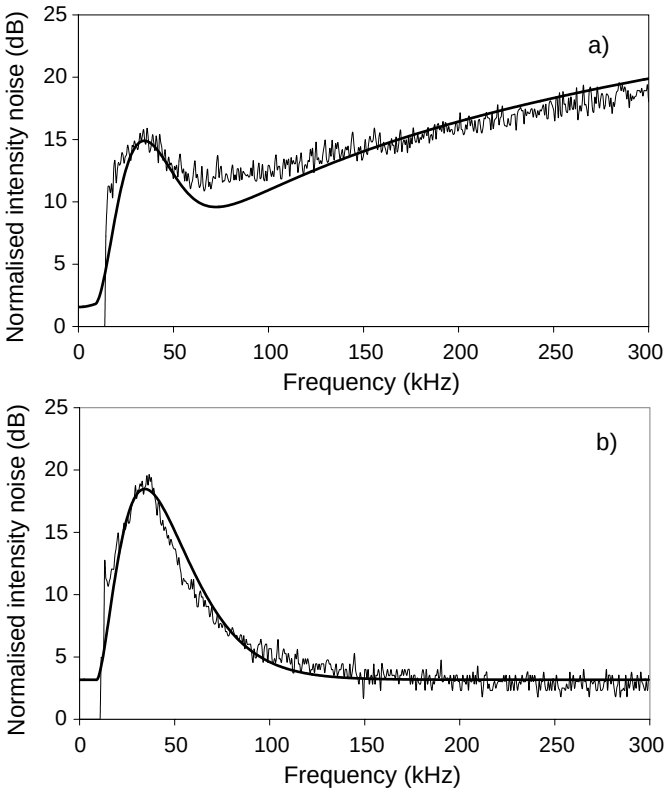

Fig. 5. a) Normalised experimental and theoretical (thick line) intensity noise spectra of the Nd:YVO_4 microchip laser pumped by a noisy grating extended cavity laser diode in the 0–300 kHz frequency range. The corresponding pump noise is shown in b. b) Normalized intensity noise spectrum of the noisy grating extended cavity laser diode in the low-frequency region (0–300 kHz). The fit (thick line) is obtained with an empirical expression.

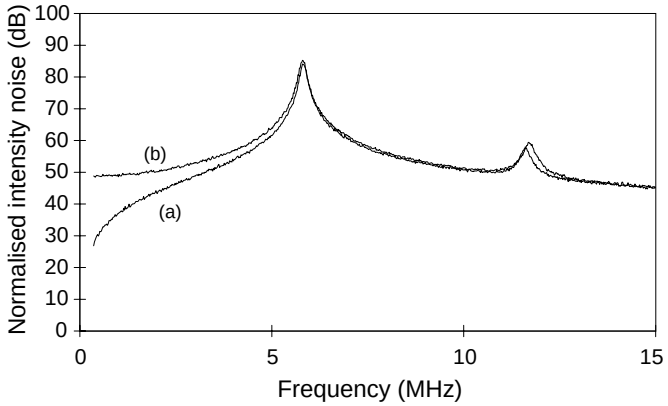

Fig. 6. Normalised intensity noise spectra of the Nd:YVO_4 microchip laser for a squeezed pump (curve (a)) and for a noisy pump with an excess noise of more than 40 dB (curve (b)).

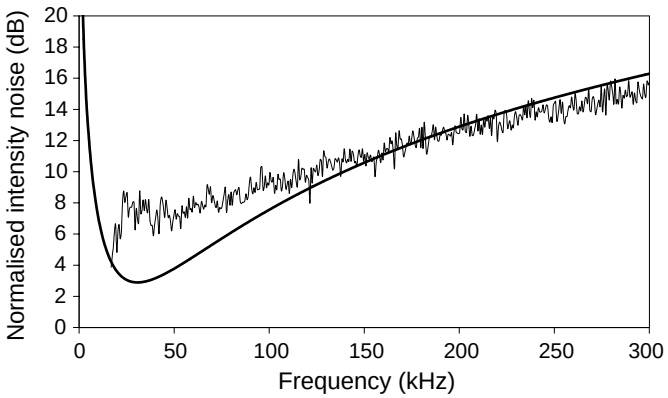

Fig. 7. Normalised experimental and theoretical (thick line) intensity noise spectra of the Nd:YVO_4 microchip laser pumped by an injection locked laser diode in the 0–300 kHz frequency range.

between the total intensity noise and the noise of the main mode alone: side modes are actually negligible and single-mode squeezing is generated. Thus, when pumped with a grating extended cavity laser, Nd:YVO_4 microchip laser does not experience any excess pump noise; nevertheless, extra noise in the low-frequency region is observed.

To further check the origin of the excess noise, we performed a noise measurement on the Nd:YVO_4 microchip laser in the same conditions as Figure 4, except for the pump noise, that exhibit a large excess noise peak up to 20 dB centered at 40 kHz, as shown in Figure 5b. The corresponding theoretical and experimental intensity noise spectrum of the microchip laser can be seen in Figure 5a. The peak of the pump noise is very well reproduced in the noise of the microchip laser. In this case the agreement between theory and experiment is good also at low frequencies. Other measurements performed with a very noisy pump (more than 40 dB) clearly confirms the significant influence of the pump fluctuations on the low-frequency noise of the Nd:YVO_4 microchip laser, as shown in Figure 6. This case is very illustrative of the high noise at low frequency that is obtained when microchip lasers are pumped with laser diodes arrays.

To improve these results and to obtain a reduction of the intensity noise of the Nd:YVO_4 with respect to the minimum noise of 11 dB above SNL achieved in the experimental conditions of Figure 4, we substitute the grating extended cavity pump laser with the injection locked one. In fact, as previously explained, with this new configuration we are able to operate the laser 10 times above threshold ($r = 10$) and according with theory, we expect an improvement on the noise performances of the laser. The result is shown in Figure 7 for a quiet pump like that reported in Figure 3a. The minimum noise at 40 kHz is 7 dB above the SNL which is a significant improvement as compared to the previous case. However, the theoretical fit does not agree with experimental curve below 100 kHz.

The fact that the theoretical noise spectrum is in good agreement with the measured noise spectrum over a very large range of frequencies seems to ensure that the Langevin approach is well adapted for description of the noise features of our Nd:YVO_4 microchip laser. The problem of modeling the noise behavior of this laser arises at low frequencies as can be seen in Figures 4b and 7. A noticeable discrepancy between theory and experiment

occurs for frequencies below 100 kHz. One possible source of this low-frequency extra noise could be the presence of non-linear effects generated by the very large noise peak of the relaxation oscillation. In fact, the intensity noise fluctuations at the level of the peak are typically 80 dB above SNL, corresponding to 1–3% of the steady-state intensity. Moreover, the occurrence of non-linear effects is clearly demonstrated by the presence of the harmonic of the relaxation oscillation peak (Fig. 4b). We have carefully checked the linearity of our detection system in the overall range of detected powers, in order to exclude other possible causes of the observed harmonic as non-linearities or saturation effects in any photodetection stage.

The theoretical noise spectrum obtained by linearisation of the stochastic c-number Langevin equation around the steady-state solutions does not take into account the non-linear phenomena and its derivation is valid in the case of very small fluctuations with respect to the steady-state values.

In order to investigate the possible non-linear effects at low frequency we have reduced the noise around the relaxation oscillations by an appropriate feedback loop reacting on the laser diode driving current. The feedback loop has a tailored frequency response in order to be active only in a narrow frequency region around the peak, while keeping unchanged the noise features of the laser at low frequencies. Nevertheless, we observed a sharp reduction (typically 5–7 dB) of the intensity noise at low frequencies. Although the feedback loop does not affect the low-frequency part of the spectrum, the low-frequency noise is now in agreement with the theoretical predictions. This behaviour that gives a strong indication for non-linear effects will be studied in detail in a forthcoming paper.

5 Conclusion

In this work, we have presented a detailed investigation of the intensity noise of a Nd:YVO_4 microchip laser pumped by an amplitude squeezed laser diode. The squeezed light pump is obtained with two different configurations: grating extended cavity laser and injection locked laser. We have clearly demonstrated the effect of the reduced pump noise on the low-frequency region of the intensity noise spectrum of the microchip laser. The sub-shot noise operation of the pump laser diode allows to achieve an intensity noise of 7 dB above SNL at 40 kHz, considerably reduced with respect to the performances achievable with pumping by standard laser diodes which present excess pump noise of typically 20 dB at low frequencies. The theoretical intensity noise spectra calculated from a full quantum model based on quantum Langevin approach are in very good agreement with experimental observations, except for very low frequencies ($<$ 100 kHz). This extra low-frequency noise may be a consequence of a non-linear effect due to the strong relaxation oscillation peak.

In conclusion, our analysis shows that the Nd:YVO_4 microchip laser could potentially exhibit sub-shot noise operation in the low-frequencies region. At present, two dominant factors prevent to achieve noise reduction below SNL in this laser. On the one hand, the pump laser diode exhibits a slight excess noise in the low-frequency range ($<$ 300 kHz), where the microchip laser should take more relevant advantages from pump noise reduction, as shown by theoretical analysis. On the other hand, the previously described non-linear effects increase the noise in the same low-frequency range. Therefore improvement on low-frequency noise of the pump laser diode, together with specially designed feedback loop to eliminate extra low-frequency noise, are necessary to a further reduction of the intensity noise of the Nd:YVO_4 microchip laser.

Thanks are due to A.Z. Khoury and F. Marin for useful discussions. This research was carried out in the framework of the EC ESPRIT Contract ACQUIRE no. 20029 and of the EC TMR microlasers and cavity QED program (Contract no. ERBFMRXCT 96-00066). One of us (A.B.) had the support of a TMR fellowship no. ERBFMBI CT950204.

Appendix

We report the non-vanishing diffusions coefficients for the c-number Langevin forces:

$$2\mathcal{D}_{aa} = (\gamma_a + \gamma'_a)\,\langle \mathcal{N}_a(t)\rangle + R(1-p) - g\,[\langle \mathcal{M}^*(t)\mathcal{A}(t) + \mathcal{A}^*(t)\mathcal{M}(t)\rangle]\,, \quad \text{(A.1)}$$

$$2\mathcal{D}_{bb} = \gamma_b\,\langle \mathcal{N}_b(t)\rangle + \gamma'_a\,\langle \mathcal{N}_a(t)\rangle - g\,[\langle \mathcal{M}^*(t)\mathcal{A}(t) + \mathcal{A}^*(t)\mathcal{M}(t)\rangle]\,, \quad \text{(A.2)}$$

$$2\mathcal{D}_{ab} = -\gamma'_a\,\langle \mathcal{N}_a(t)\rangle + g[\langle \mathcal{M}^*(t)\mathcal{A}(t) + \mathcal{A}^{*(t)\mathcal{M}}(t)\rangle], \quad \text{(A.3)}$$

$$2\mathcal{D}_{\mathcal{M}\mathcal{M}} = 2g\,\langle \mathcal{M}(t)\mathcal{A}(t)\rangle\,, \quad \text{(A.4)}$$

$$2\mathcal{D}_{\mathcal{M}^*\mathcal{M}} = (2\gamma_{ab} - \gamma_a - \gamma'_a)\,\langle \mathcal{N}_a(t)\rangle + R\,, \quad \text{(A.5)}$$

$$2\mathcal{D}_{b\mathcal{M}} = \gamma_b\,\langle \mathcal{M}(t)\rangle\,. \quad \text{(A.6)}$$

References

1. A.C. Nilsson, IEEE J. Quantum Electron. **25**, 767 (1989).
2. A. Arie, S. Schiller, E.K. Gustafson, R.L. Byer, Opt. Lett. **17**, 1204 (1992).
3. C.C. Harb, T.C. Ralph, E.H. Huntington, I. Freitag, D.E. McClelland, H.-A. Bachor, Phys. Rev. A **54**, 4370 (1996).
4. T.C. Ralph, C.C. Harb, H.-A. Bachor, Phys. Rev. A **54**, 4359 (1996).

5. E.H. Huntington, B.C. Buchler, C.C. Harb, T.C. Ralph, D.E. McClelland, H.-A. Bachor, Opt. Commun. **145**, 359 (1998).
6. Yu. M. Golubev, I.V. Sokolov, Zh. Eksp. Teor. Phys. **87**, 804 (1984) (Sov. Phys. JETP **60**, 234 (1984)).
7. Y. Yamamoto, S. Machida, O. Nilsson, Phys. Rev. A **34**, 4025 (1986).
8. M.J. Freeman, H. Wang, D.G. Steel, R. Craig, D.R. Scifres, Opt. Lett. **18**, 2141 (1993).
9. H. Wang, M.J. Freeman, D.G. Steel, Phys. Rev. Lett. **71**, 3951 (1993).
10. M J. Freeman, H. Wang, D.G. Steel, R. Craig, D.R. Scifres, Opt. Lett. **18**, 379 (1993).
11. C. Becher, K.-J. Boller, Opt. Commun. **147**, 366 (1998).
12. M.I. Kolobov, L. Davidovich, E. Giacobino, C. Fabre, Phys. Rev. A **47**, 1431 (1993).
13. N.B. Abraham, P. Mandel, L. Narducci, *Dynamic Instability and Pulsations in Lasers*, in *Progress in Optics*, edited by E. Wolf (Elsevier, Amsterdam, 1988).
14. T. Taira, A. Mukai, Y. Nozawa, T. Kobayshi, Opt. Lett. **16**, 1955 (1991).
15. T.-C. Zhang, J.-Ph. Poizat, P. Grelu, J.-F. Roch, P. Grangier, F. Marin, A. Bramati, V. Jost, M.D. Levenson, E. Giacobino, Quantum Semiclass. Opt. **7**, 601 (1995).
16. W. Koechner, *Solid State Laser Engineering*, second edition (Springer Verlag, Berlin, 1988).
17. A. Kaminskii, *Laser Crystals*, second edition (Springer Verlag, Berlin, 1981).
18. F.E. Hovis, M. Stuff, C.J. Kennedy, B. Vivian, IEEE J. Quantum Electron. **28**, 39 (1992).
19. F. Marin, A. Bramati, E. Giacobino, T.-C. Zhang, J.-Ph. Poizat, J.-F. Roch, P. Grangier, Phys. Rev. Lett. **75**, 4606 (1995).